

CBPF-NF-015/90

MEASUREMENT OF FISSION YIELDS USING TARGET MATERIALS IN
CONTACT WITH SOLID STATE TRACK DETECTORS

by

O.A.P. TAVARES

Centro Brasileiro de Pesquisas Físicas - CBPF/CNPq
Rua Dr. Xavier Sigaud, 150
22290 - Rio de Janeiro, RJ - Brasil

A method to evaluate fission yields in experiments of induced and spontaneous fission which use fissionable target materials in the configuration of contact with dielectric track detectors has been developed. The effect of energy absorption of the fission fragments by the target sample, and the optical resolution power for observation of etched fission tracks are taken into account in deducing the total efficiency factors resulting from the use of targets of different thicknesses. With this method, the conditions to give the maximum observable density of etched tracks can be obtained, which is important to experiments of low fission yields. A number of useful formulae applicable to mica and plastic track detectors for evaluation of fission yields are reported. The method has been successfully applied to recent photo-fission experiments of low fission yields, and it can also be useful in the study of other fission cases as well as in applications to fission-related problems.

Key words: fission fragments, track-etch detectors, fission yields, energy-loss rate, thin and thick targets, recording efficiency.

Running head: Measurement of fission yields.

1 INTRODUCTION

During the last two decades or so, solid state nuclear track detectors (SSNTD) have been used extensively as fission fragment detectors in studies of different cases of fission phenomena (spontaneous and induced fission) of complex nuclei and related topics, as well as in many applications to related modern nuclear disciplines (fission track dating, uranium content of materials and distribution, and other)^{1,2}. The most common configuration that has been used in fission experiments and applications consists of contacting a target sample material with an appropriate dielectric detector (micas, polymers, polycarbonates). If the target is a very thin one, i.e., the target thickness x_0 involved is a very small fraction of the average residual range \bar{a}_0 of the median fission fragment in the target material ($x_0 \ll \bar{a}_0$), the effect of fragment absorption by the target itself may be considered rather negligible and, in this case, the etching efficiency ϵ_e is dictated by the critical angle of etching, ϕ_c , through the well known relationship $\epsilon_e = 1 - \sin\phi_c$, and the "effective" thickness of the target is simply equal to x_0 . Another extreme situation is encountered whenever one uses thick targets ($x_0 > \bar{a}_0$) placed in intimate contact with a fission track detector. In this case, it has been shown that the etching efficiency is given by $\epsilon_e = \cos^2\phi_c$, and the "effective" target thickness turns out to be $\bar{a}_0/2$ (see, for instance, Ref. 2).

The etching (or registration) efficiencies mentioned above, however, should be thought as "ideal" efficiency factors

since they have been calculated under the assumption of constant track etch rate, v_T , at all points along the track, an assumption which is not verified rigorously in practice during the etching of fission fragment tracks. Besides, visualization and identification of etched tracks under an optical microscope depend strongly upon the resolution power of the optical system used for observation of tracks, in the sense that not all the tracks revealed by etching are actually observed. This makes the evaluation of an additional efficiency factor related to observation (identification) of the etched fission tracks, ω , necessary. For a very thin target placed in contact with a fission track detector it is straightforward to obtain that

$$\omega = \frac{1 - \frac{\sin\phi_c}{1-r/\bar{R}}}{1 - \sin\phi_c}, \quad (1)$$

where r and \bar{R} are, respectively, the minimal and the average maximum etched fission track lengths observed. Since r can be as small as $\sim 3\mu\text{m}$ under usual conditions of optical resolution, $\phi_c \lesssim 5^\circ$ for fission fragment detectors such as mica, makrofol, lexan and CR-39, and \bar{R} varies in the interval $\sim 10\text{-}18\mu\text{m}$ for most fissionable target materials, it results that $\omega \gtrsim 0.96$ (of course, both \bar{R} and ϕ_c depend on etching conditions; the values quoted here refer to usual, normal etching conditions for fission fragments¹). For thick targets in 2π -geometry the observation efficiency results to be

$$\omega = 1 - \frac{r}{\bar{R}}, \quad (2)$$

as it was deduced in Ref. 3. The total, combined efficiency is

clearly given by ϵ_e^ω .

The evaluation of the efficiency factors by means of expressions (1) and (2) imposes measurement of etched track lengths in order to obtain the values for the quantities r and \bar{R} . As track-length measurements are in general time consuming we were led to develop a new method which allows one to obtain the correct number of fission events from the actual number of etched fission tracks observed (and so the fission yield) in fission experiments whenever a track detector is used in the configuration of intimate contact with a fissionable target material. The method is based on knowledge of the following quantities: i) actual thickness of the target sample (x_0); ii) minimal track-length projection possible of being observed (p); iii) thickness of detector surface removed out by etching ($v_G t$, where v_G is the general etch rate of the undamaged detector material, and t is the etching time), and iv) average full residual ranges of fission fragments (\bar{a}_0 and \bar{r}_0), respectively, in the target and detector materials. The present study was motivated by the necessity of evaluating low-energy fission yields of a number of target nuclei induced by monochromatic and polarized photon beams in the incident energy interval of ~ 40 -80MeV, where different dielectric materials have been used as fission track detectors^{4,5}. The aim of the present work is to present and discuss to some detail the method developed by us which gives an alternative way to evaluate fission yields.

2 FORMULATION OF THE PROBLEM AND BASIC ASSUMPTIONS

In induced fission experiments which use extended target samples (metal foils, films, etc), the fission yield (or cross section, σ) is obtained by

$$\sigma = \frac{N_e}{QN_a} \quad , \quad (3)$$

where N_e is the number of fission events occurred per unit volume of the sample, N_a is the number of fissionable target nuclei per unit volume, and Q is the number of particles incident perpendicularly per unit area, provided the values of σ and N_a are such that they do not produce any significant attenuation on incident particle beam. If a dielectric track detector is placed in contact with a fissionable target sample material (a configuration termed 2π -geometry) only a fraction of the N_e fission events will be recorded on the detector surface. This, after being revealed by etching, will produce a number N_t of fission tracks observed per unit area. The arrangement is shown schematically in Figure 1a. The question is to know how the quantities N_t and N_e are related to each other in order to obtain σ by means of equation (3). The relationship between N_t and N_e will depend on sample thickness, the rate of energy-loss of fission fragments in both target and detector materials, the etching conditions used for track revelation, and the resolution power of the optical system for observation of the etched fission tracks. To simplify the calculation, it will be considered the following basic assumptions:

- i) The target sample is homogeneous and uniform, and nuclear fragments are emitted isotropically from any point inside the sample; the distribution of fission fragments is replaced by its most probable (or median) fission mode;
- ii) Latent fission tracks are revealed by etching for fission fragments entering the detector at angles greater than their critical angles of etching (measured from the detector surface);
- iii) The threshold of observation of etched tracks is defined by a certain minimal track-length projection, p , allowed by the resolution power of the optical system; good definition of track image imposes the condition $v_T \gg v_G$ during etching, a condition which is verified for micas and most plastics;
- iv) Since the kinetic energy of fission fragments is low ($\lesssim 1$ MeV/u), the rate of energy-loss (due essentially to ionization) in both the target and detector materials can be described by simple relationships of the form^{6,7}

$$-\frac{dE}{dy} = \xi_a E^\beta \quad , \quad -\frac{dE}{dy} = \xi_d E^\beta \quad , \quad (4)$$

where E is the fragment kinetic energy, and ξ_a , ξ_d , and β are constants (the subscripts a and d denote, respectively, the target and detector). The constant β ($0 < \beta < 1$) may be considered as much as the same for both media, and $\xi_a > \xi_d$. It follows from (4) that the residual ranges will be given by

$$R_a(E) = \frac{E^{1-\beta}}{\xi_a(1-\beta)} \quad , \quad R_d(E) = \frac{E^{1-\beta}}{\xi_d(1-\beta)} \quad , \quad (5)$$

and the average full residual ranges, respectively, in the target sample and detector media will be given by

$$\bar{a}_0 = R_a(E_0) \quad , \quad \bar{r}_0 = R_d(E_0) \quad , \quad (6)$$

where E_0 is the initial kinetic energy of the median fission fragment.

The calculation will proceed in its general form, i.e., irrespective of the target thickness. Different practical situations of very thin ($x_0 \ll \bar{a}_0$), thin ($x_0 < \bar{a}_0$), and thick ($x_0 \geq \bar{a}_0$) targets will be discussed separately from the general solution.

3. DERIVATION OF THE YIELD FORMULA AND DISCUSSION

Consider a fission fragment which moves towards the detector with an initial kinetic energy E_0 from a point-origin inside the sample, the position of which given by the vertical distance x from the target-detector interface (Figure 1b). First, the fragment travels a distance a inside the target sample, reaching the interface with an energy $E < E_0$, and then it penetrates the detector where it travels a path-length r before coming to rest. Denoting the dip angle by ϕ , from equations (5) and (6) and Figure 1b, we have

$$x = \bar{a}_0 \left(1 - \frac{r}{\bar{r}_0} \right) \sin\phi \quad . \quad (7)$$

Since each fission event produces two fragments moving apart, the number of fission fragments emitted from a sample layer of

-7-

thickness dx and within the solid angle $d\Omega = 2\pi\cos\phi d\phi$ is given by

$$\frac{d^2N}{d\Omega dx} = \frac{N_e}{4\pi} \times 2 \quad , \quad (8)$$

and, therefore,

$$d^2N = N_e \cos\phi d\phi dx \quad . \quad (9)$$

Integration of (9) between the limits allowed for ϕ and x will give the final number of etched fission tracks that are revealed by etching and observed per unit area of the detector surface, i.e.,

$$N_t = N_e \int_0^{x_M} \int_{\phi_1}^{\phi_2} \cos\phi d\phi dx = N_e \int_0^{x_M} (\sin\phi_2 - \sin\phi_1) dx \quad , \quad (10)$$

where ϕ_1 and ϕ_2 are the dip angles which allow for visualization of tracks down to the threshold track-length projection (p), and x_M (the maximum of x) is such that a fission fragment which has entered the detector can still be revealed and observed.

The limiting values x_M , ϕ_1 , and ϕ_2 can be evaluated with the aid of Figure 2, where all quantities necessary to calculation have been depicted. From inspection of Figure 2 we have

$$r = \frac{p}{\cos\phi} + \frac{v_G t}{\sin\phi} \quad , \quad (11)$$

which combines with equation (7) to give

$$f(u) = u - A - \frac{Bu}{\sqrt{1-u^2}} = 0 \quad , \quad (12)$$

with

$$u = \sin\phi \quad (13)$$

$$A = \frac{x}{\bar{a}_0} + \frac{v_G t}{\bar{r}_0} \quad (14)$$

$$B = \frac{p}{\bar{r}_0} \quad (15)$$

The solutions of equation (12) in the interval $0 < u < 1$ give the values of $\sin\phi_1$ and $\sin\phi_2$ to be inserted into equation (10). These are illustrated in Figure 3 for an actual case of a metallic bismuth target placed in contact with a makrofol detector (this example was taken from a recent photofission experiment conducted within the scope of a collaboration programme on low-energy photofission reactions⁵). It is seen from Figure 3 that equation (12) has two solutions only for values of x in the interval $0 \leq x < x_M$, where x_M is obtained from the condition $f(u)_{\max} = 0$. Solving for x_M , it is straightforward to obtain that

$$x_M = \bar{a}_0 \left\{ \left[1 - \left(\frac{p}{\bar{r}_0} \right)^{2/3} \right]^{3/2} - \frac{v_G t}{\bar{r}_0} \right\} \quad (16)$$

If the actual target thickness x_0 is less than x_M , equation (12) has solutions only for $0 \leq x \leq x_0$. As x increases from 0 up to x_M (or x_0), the difference $\sin\phi_2 - \sin\phi_1 = \epsilon(x)$ decreases from $\epsilon_0 = \epsilon(0)$ down to 0 (or $\epsilon(x_0)$). The quantity

$$\epsilon_0 = \left[\sin\phi_2 - \sin\phi_1 \right]_{x=0} \quad (17)$$

is just the total, combined efficiency factor for an ideal, null

target sample thickness. An evaluation of ϵ_0 can be obtained as follows. We see that for $u = \sin\phi \ll 1$, equation (12) gives $\sin\phi_1 = A/(1-B)$. Next, starting from the approximate solution $\sin\phi_2 \approx (1-B^2)^{1/2}$, we can solve (12) to a better approximation to obtain

$$\sin\phi_2 = (1-B^2)^{1/2} - \frac{A}{1/B^2-1} \quad (18)$$

and, finally,

$$\epsilon_0 = (1-B^2)^{1/2} - \frac{A(B^2+B+1)}{1-B^2} \quad (19)$$

Numerical calculations have indicated that the difference $\sin\phi_2 - \sin\phi_1 = \epsilon(x)$ can be described to a good approximation by a function of the form

$$\epsilon(x) = \epsilon_0 \left(1 - \frac{x}{x_M}\right)^\alpha, \quad 0 < \alpha < 1 \quad (20)$$

Since equation (19) applies also to small values of x ($x \lesssim 1\mu\text{m}$), the exponent α can be evaluated by equating the derivatives of $\epsilon(x)$ at $x = 0$ obtained from (19) and (20), i.e.,

$$\frac{d}{dx} \left[(1-B^2)^{1/2} - \frac{A(B^2+B+1)}{1-B^2} \right] \Big|_{x=0} = \frac{d}{dx} \left[\epsilon_0 \left(1 - \frac{x}{x_M}\right)^\alpha \right] \Big|_{x=0}, \quad (21)$$

which gives

$$\alpha = \frac{1}{\epsilon_0} \frac{x_M}{a_0} \frac{B^2+B+1}{1-B^2} \quad (22)$$

It should be remarked that the relationships (19), (20), and (22)

are approximations constructed to replace the solutions of equation (12), which can be obtained to a high degree of accuracy by using numerical calculations. The uncertainties in the quantities \bar{a}_0 , \bar{r}_0 , p , and $v_G t$ make this approximate, analytical method appropriate in deducing the subsequent quantities of interest. With this observation in mind, we can now integrate (10) by making use of (20), where the two following different cases must be considered:

i) $x_0 \geq x_M$. In this case, the maximum of x is x_M , and equation (10) gives

$$N_t = \frac{N_e x_M^\epsilon \epsilon_0}{\alpha + 1} \quad . \quad (23)$$

ii) $x_0 < x_M$. Here, the maximum of x is obviously x_0 , and equation (10) gives

$$N_t = \frac{N_e x_M^\epsilon \epsilon_0}{\alpha + 1} \left[1 - \left(1 - \frac{x_0}{x_M} \right)^{\alpha + 1} \right] \quad . \quad (24)$$

Inserting these two results into the general expression for the cross section (equation (3)), one obtains

$$\sigma = \frac{N_t}{Q N_a \frac{x_M^\epsilon \epsilon_0}{\alpha + 1}} \quad , \quad x_0 \geq x_M \quad (25)$$

and

$$\sigma = \frac{N_t}{Q N_a \frac{x_M^\epsilon \epsilon_0}{\alpha + 1} \left[1 - \left(1 - \frac{x_0}{x_M} \right)^{\alpha + 1} \right]} \quad , \quad x_0 < x_M \quad . \quad (26)$$

It is noticed that a target sample having a thickness $x_0 = x_M$ will produce the maximum number of tracks observed per unit area of the detector surface,

$$(N_t)_{\max} = \frac{\sigma Q N_a x_M \epsilon_0}{\alpha + 1} \quad , \quad (27)$$

which is an important result to statistical considerations of low fission-yield experiments.

Since the essential quantities related to the fission track-etch method which will give ultimately the total number of etched fission tracks to be observed (and so, the fission yield) are x_M , ϵ_0 and α , it is instrutive to see how these quantities vary with p for fixed etching conditions ($v_G t$ constant). We choose the same parameter values of an actual fission yield experiment as quoted in Figure 3. Figure 4 shows the variation of the referred quantities within a range of p -values of routine use. It is seen a significant decreasing of x_M , ϵ_0 and α , as well as of the quantity $x_M \epsilon_0 / (\alpha + 1)$, as the optical resolution diminishes, therefore reducing the total number of tracks observed and, thus, leading to poor statistics. For the example under consideration, the present analytical method gives values of fission yield which differs from the exact solution by a maximum of 3%.

Finally, let us discuss the present results by considering the different ranges of target sample thickness, x_0 . To simplify the discussion, we will define the type of a target sample by comparing x_0 with x_M , and not with \bar{a}_0 as usual.

i) Very thin targets ($x_0 \ll x_M$). For such target samples, $x_0 \ll \bar{a}_0$ too. From equation (26), we have

$$\sigma = \frac{N_t}{QN_a x_0 \epsilon_0} \quad (28)$$

The "effective" target thickness is x_0 , and the total efficiency is

$$\epsilon_{\text{very thin}} = \epsilon_0 \quad (29)$$

which is given by (19). Note that if the optics was not taken into account, i.e., $p = 0$, we would have $\epsilon_0 = 1 - v_G t / \bar{r}_0$. Since for a full-range etched track $\bar{r}_0 \approx v_T t$, it follows that $\epsilon_0 \approx 1 - v_G / v_T = 1 - \sin \phi_c$, which is the commonly used expression for the efficiency.

ii) Thin targets ($x_0 < x_M$). In this case we may interpret $x_M / (\alpha + 1)$ in equation (26) as the "effective" target thickness, and the quantity

$$\epsilon_{\text{thin}} = \left[1 - \left(1 - \frac{x_0}{x_M} \right)^{\alpha+1} \right] \epsilon_0 \quad (30)$$

as the total efficiency.

iii) Thick targets ($x_0 \geq x_M$). Here, equation (25) is applicable and, by using the expression for x_M , we may define

$$\epsilon_{\text{thick}} = \left\{ \left[1 - \left(\frac{p}{\bar{r}_0} \right)^{2/3} \right]^{3/2} - \frac{v_G t}{\bar{r}_0} \right\} \epsilon_0 \quad (31)$$

as the total efficiency, and the quantity $\bar{a}_0 / (\alpha + 1)$ as the "effective" target thickness. It should be noted that if a threshold track-length projection for track visualization was not defined ($p=0$) ϵ_{thick} would be given by $(1 - \sin \phi_c)^2$, where ϕ_c applies to fission fragments originated from a sample layer

in contact with the detector surface ($x \approx 0$). This result differs from $\cos^2 \phi_c$ because the former has been obtained by taking into account the energy absorption effect of fission fragments along their path-length inside the sample (cf. equations (5-7)), whereas the latter one emerges under the assumption of ϕ_c constant, i.e., v_T constant for fragments originated either from near the detector surface or deeper target layers.

Results discussed above apply also to spontaneous fission case and applications. It suffices to replace the quantity σQ by the new one, $\lambda \tau$, where λ denotes the decay constant, and τ is the exposure time.

Finally, to practical use of the method developed in the present work it is required evaluation of the chief quantities \bar{a}_0 , \bar{r}_0 , $v_G t$, and p . The two first ones can be evaluated from available range-energy tables⁶⁻⁹, or calculated from appropriate computer codes like the one reported in reference 2. Estimates of kinetic energy of fission fragments for different fission cases of interest can be obtained from empirical correlations such as the classical one reported by Viola, Jr.¹⁰. The quantity $v_G t$ is easily measured directly by the current etching methods, and calibrated eye-pieces fitted out to oculars of routine use in ordinary microscopy allow for the determination of p .

4 SUMMARY AND CONCLUSIONS

The use of fissionable target sample materials in contact with dielectric track detectors of high detection efficiency, such as micas and plastics, is a suitable arrangement for

measuring absolute fission yields in both induced and spontaneous fission experiments. Fission yield formulae which incorporate the main correction factors due to energy absorption effects of fission fragments by the target material, and the optical resolution power for observation of etched fission tracks have been deduced. These formulae give results to a sufficient degree of accuracy, and, if necessary, more accurate results can be obtained by developing numerical calculations. Target samples have been classified according to thickness, and expressions for total efficiency (etching efficiency times observation efficiency) have been obtained. Of special importance to low fission yield experiments are the conditions which may be used to obtain the best (from a statistical point of view) result for track counting. It has been shown how the optics to be used in track analysis can serve as a guide in choosing the most adequate target thickness to give the maximum density of etched fission tracks. The method developed in the present work can easily be extended and applied to similar experimental problems, such as natural or induced emission of nuclear fragments, and other nuclear reaction studies as well.

ACKNOWLEDGEMENT

The author wishes to thank J.B. Martins, E.L. Moreira, J.D. Pí-nheiro Filho, and J.L. Vieira for valuable discussions. The partial support by the Brazilian Financiadora de Estudos e Projetos-FINEP is gratefully acknowledged.

FIGURE CAPTIONS

FIGURE 1 a) Schematic representation of a target material and a solid state nuclear track detector in the configuration of contact to measure induced fission yields. b) Trajectory of a nuclear fragment from a point-origin inside the target and crossing the target-detector interface.

FIGURE 2 Defining the different geometrical quantities of etched fission tracks as used throughout the text.

FIGURE 3 Illustrating the solutions of equation (12) for different values of target thickness, x . It is shown the case of a Bi-target in contact with a makrofol fission-track detector, for which case $\bar{a}_0 = 11.5\mu\text{m}$ and $\bar{r}_0 = 16\mu\text{m}$, $v_{Gt} = 0.73\mu\text{m}$, and it is assumed $p = 4.0\mu\text{m}$.

FIGURE 4 Showing the dependence of the quantities x_M , ϵ_0 and α with the optical resolution power represented by the minimal observed track-length projection, p . Experimental conditions are indicated (for details, see text).

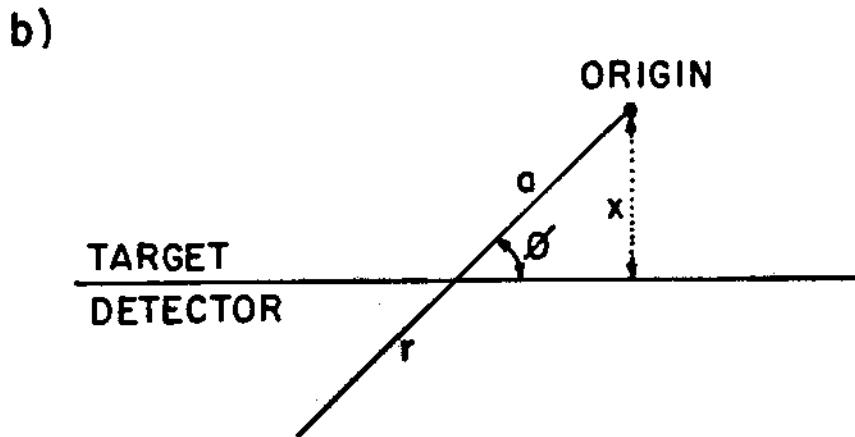
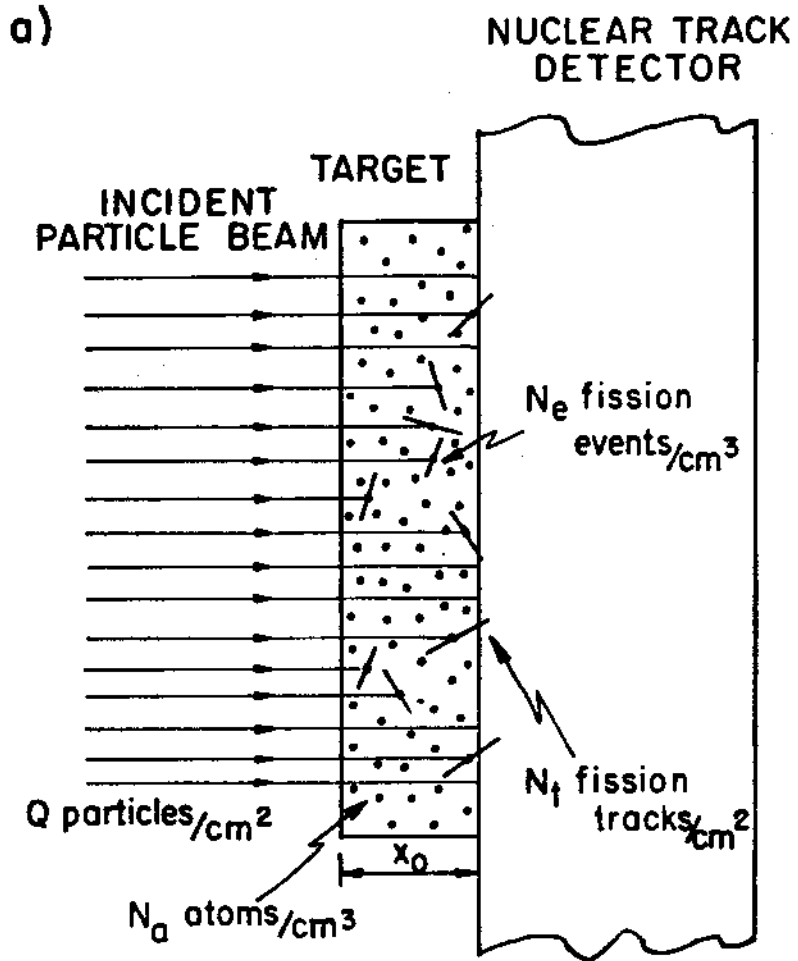


Fig. 1

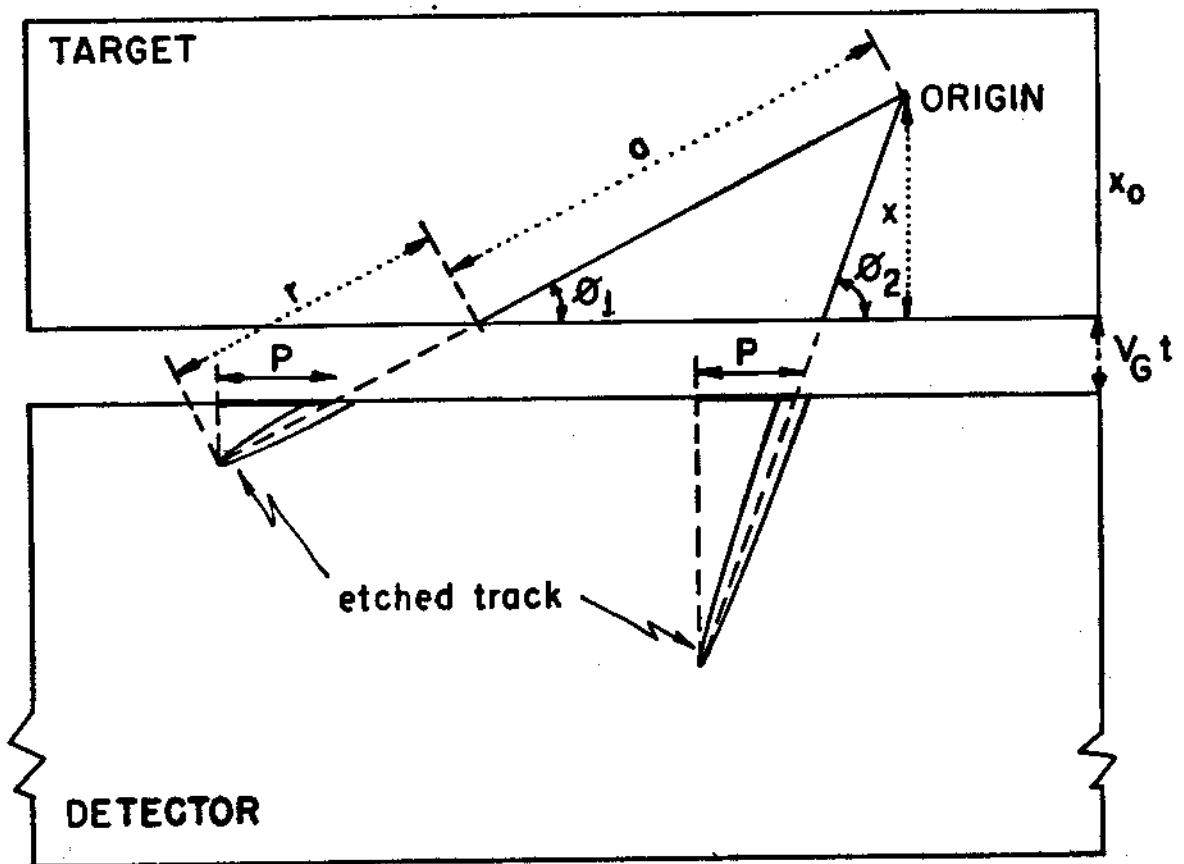


Fig. 2

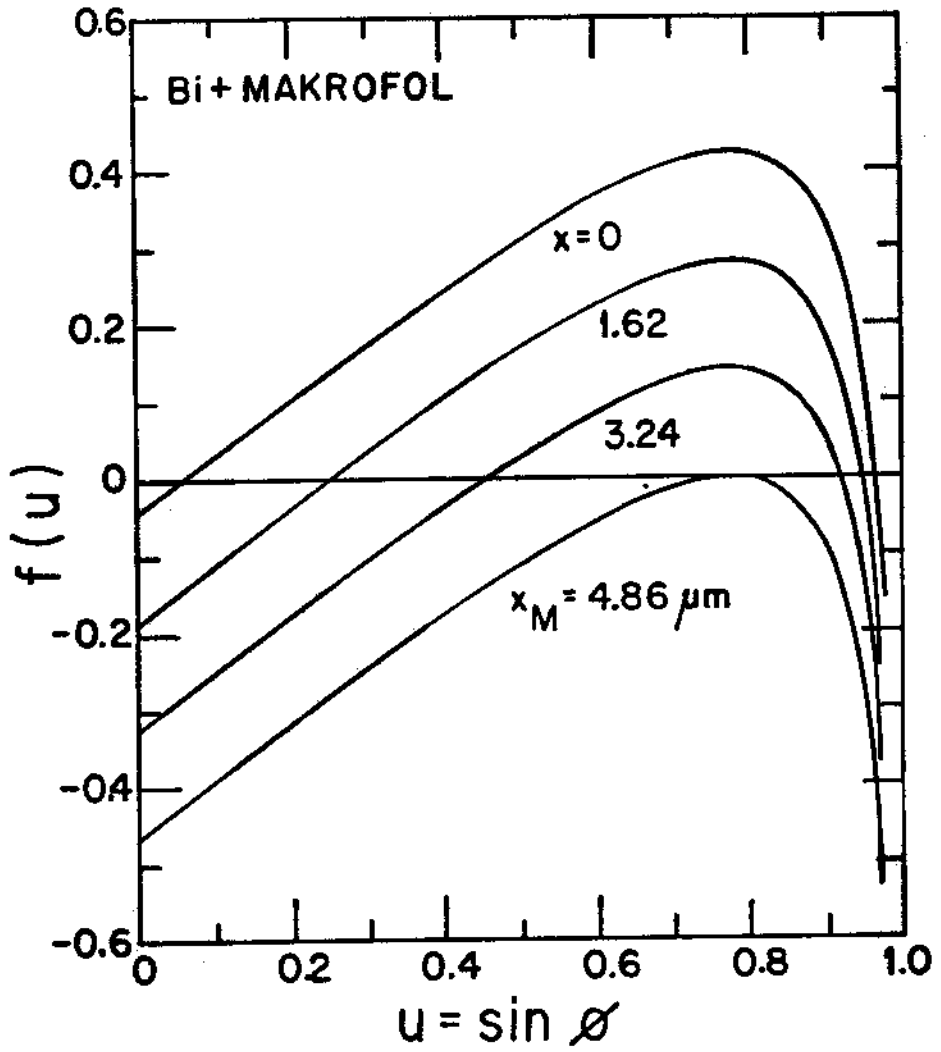


Fig. 3

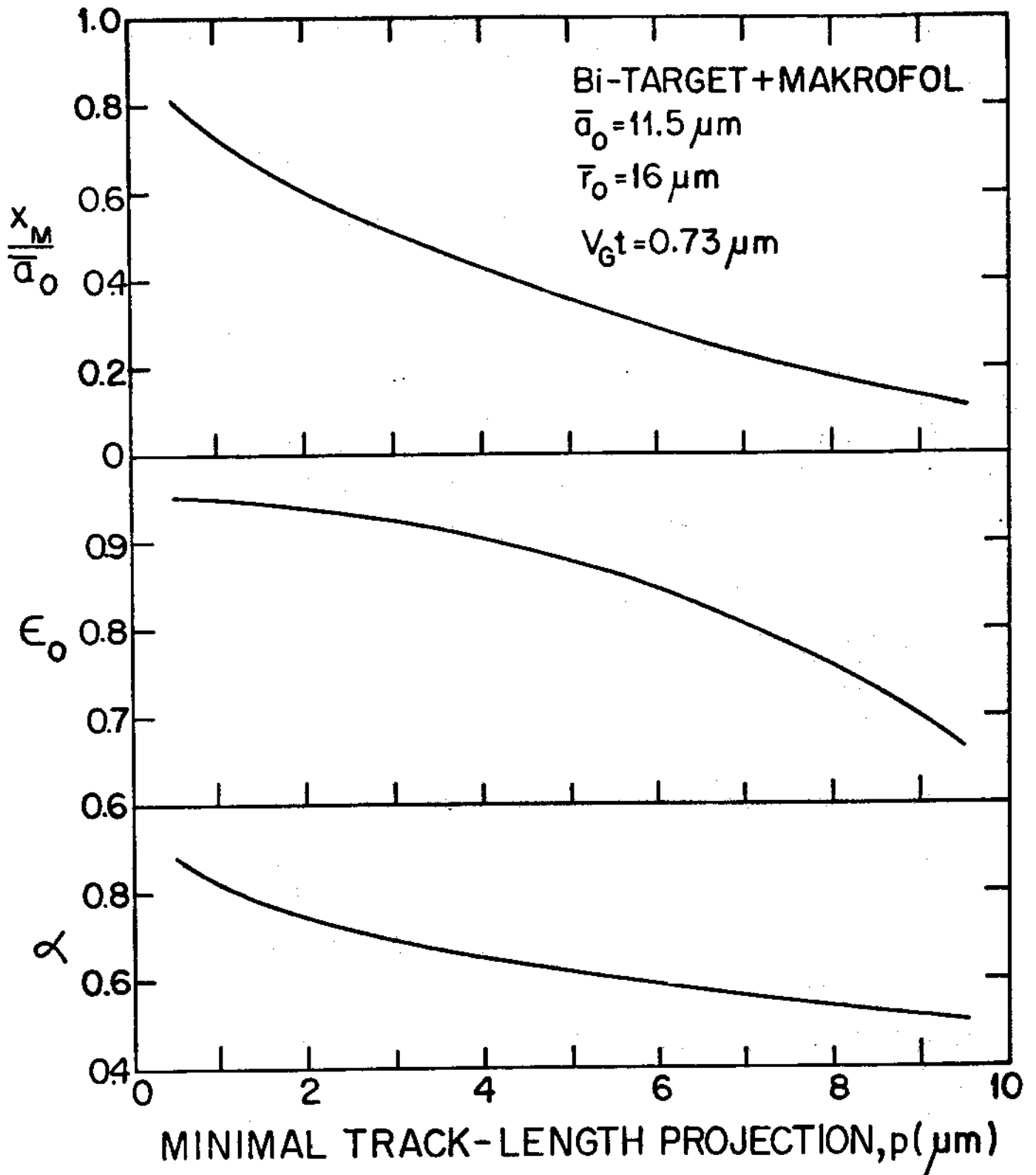


Fig. 4

REFERENCES

1. R.L. Fleischer, P.B. Price, and R.M. Walker, *Nuclear Tracks in Solids: Principles and Applications* (University of California Press, Berkeley, 1975), 1st ed.
2. S.A. Durrani and R.K. Bull, *Solid State Nuclear Track Detection: Principles, Methods and Applications* (Pergamon Press, Oxford, 1987), 1st ed.
3. D.A. de Lima, J.B. Martins, and O.A.P. Tavares, *Nucl. Instr. and Meth. in Phys. Res.* B30,67(1988).
4. R. Bernabei, V.C. de Oliveira, J.B. Martins, O.A.P. Tavares, J.D. Pinheiro Filho, S. D'Angelo, M.P. De Pascale, C.Schaerf, and B. Girolami, *Nuovo Cimento* 100A,131(1988).
5. J.B. Martins, E.L. Moreira, O.A.P. Tavares, J.L. Vieira, J. D. Pinheiro Filho, R. Bernabei, S. D'Angelo, M.P. De Pascale, C. Schaerf, and B. Girolami, *Nuovo Cimento* 101A,789(1989).
6. J. Tripier, G. Remy, J. Ralarosy, M. Debeauvais, R. Stein, and D. Huss, *Nucl. Instr. and Meth.* 115,29(1974).
7. Gy. Almási and G. Somogyi, *Atomki Közlemények* 23,99(1981).
8. L.C. Northcliffe and R.F. Schilling, *Nucl. Data Tables* A7,233 (1970).
9. J.F. Janni, *Atom. Data Nucl. Data Tables* 27,147(1982); 27,341 (1982).
10. V.E. Viola, Jr., *Nucl. Data* A1,391(1966).